This full text paper was peer reviewed at the direction of IEEE Communications Society subject matter experts for publication in the IEEE INFOCOM 2010 proceedings
This paper was presented as part of the main Technical Program at IEEE INFOCOM 2010.

Pattern Mutation in Wireless Sensor Deployment

Xiaole Bai*, Ziqiu Yun†, Dong Xuan*, Weijia Jia‡ and Wei Zhao§

*Dept of CSE
The Ohio State University
Columbus, OH, USA
{baixia, xuan}@cse.ohio-state.edu

†Dept of Math
Suzhou University
Suzhou, P. R. China
ziqiuyun@gmail.com
corresponding author

‡Dept of CS
City University of Hong Kong
Hong Kong, P. R. China
wei.jia@cityu.edu.hk

§University of Macau
Macau, P. R. China
zhao8686@gmail.com

***Abstract*—In this paper, we study the optimal deployment pattern problem in wireless sensor networks (WSNs). We propose a new set of patterns, particularly when sensors' communication range (r_c) is relatively small compared with their sensing range (r_s), and prove their optimality among regular patterns. In this study, we discover a surprising and interesting phenomenon—*pattern mutation*. This phenomenon contradicts the conjecture presented in a previous work that there exists a universal elemental pattern among optimal pattern evolution and that pattern evolution is continuous. For example, we find mutation happens among the patterns for full-coverage and 3-connectivity when $r_c/r_s = 1.0459$, among the patterns for full-coverage and 4-connectivity when $r_c/r_s = 1.3903$, and among the patterns for full-coverage and 5-connectivity when $r_c/r_s = 1.0406$. To the best of our knowledge, this is the first time that mutation in pattern evolution has been discovered. Also, our work further completes the exploration of optimal patterns in WSNs.**

I. Introduction

A. Background and Related Work

Deployment is fundamental in the design and operation of wireless sensor networks (WSNs). For years, works in sensor deployment have heavily relied on a result presented in 1939 [12] that states that the regular triangular lattice pattern (*triangle pattern* for short) is asymptotically optimal in terms of the number of discs needed to achieve full coverage. When $r_c/r_s \geq \sqrt{3}$, the triangle pattern achieves 6-connectivity.

However, $r_c/r_s \geq \sqrt{3}$ does not always hold. As an example, while the reliable communication range of the Extreme Scale Mote (XSM) platform is 30 m, the sensing range of the acoustics sensor for detecting an All Terrain Vehicle is 55 m, and $r_c/r_s = 0.545$ [1]. In practice, the range of possible values of r_c/r_s can widely vary. The communication range r_c can be affected by operating frequency, transmission power level, environment, etc. High frequencies with low communication range have the advantages of small antenna size, frequency reuse, and low power consumption. Transmission power level is also critical. For example, the reliable communication range of the TelosB mote [19] can be adjusted to less than 1 meter using the lowest power level. Finally, the RF channel's communication range is influenced by interference, reflections, scattering, and shadowing. In practice, the reliable communication range is often 60–80% of the claimed value [25]. The sensing range r_s also varies greatly for different sensor types as well as upmarket and downmarket products. It can vary from several centimeters to tens of meters [19]–[22].

This work was supported in part by the US National Science Foundation (NSF) under grants No. CNS-0916584, CAREER Award CCF-0546668, and the Army Research Office (ARO) under grant No. AMSRD-ACC-R 50521-CI; by the National Science Foundation of China (NSFC) under grant No. 10971185; by the Research Grants Council of the Hong Kong SAR, China Nos. (CityU 114908), (CityU 114609) and CityU Applied R & D Funding (ARD-(Ctr)) No. 9681001; by the National Science Foundation (NSF) under grants No. 0963973 and No. 0963979 and by the University of Macau, and Macao Science and Technology Development Foundation. Any opinions, findings, conclusions, and recommendations in this paper are those of the authors and do not necessarily reflect the views of the funding agencies.

	$r_c/r_s < 1$	$1 \leq r_c/r_s < \sqrt{2}$	$\sqrt{2} \leq r_c/r_s < \sqrt{3}$	$\sqrt{3} \leq r_c/r_s$
1-connectivity	[10] [15]			[11]
2-connectivity				
3-connectivity		[16]		
4-connectivity			[17]	
5-connectivity		[16]		
6-connectivity	[18]			

Fig. 1. The shaded areas indicates the focus of this paper. By our work, the deployment patterns with proved optimality for all ranges of r_c/r_s that achieve full coverage and k-connectivity ($k \leq 6$) are complete.

The study of optimal deployment patterns for $r_c/r_s < \sqrt{3}$ is hard, and work remains to be done. This problem is related to the covering problem in geometry. Much work has been done on the issue of covering points in a plane using a minimum number of given geometric bodies, e.g., disks [10], [12], [15], [17], orthogonal rectangles [9], fat convex bodies [7], [18], etc. However, the computational geometry literature only considers coverage, not connectivity. This is understandable, as connectivity is a typical *networking* requirement.

In recent years, some progress has been made in exploring optimal patterns for different values of r_c/r_s that are less than $\sqrt{3}$. Fig. 1 presents the state of the art. All these works assume a disc model for both sensing and communication. In 2005, the triangle pattern was shown to be non-optimal; the strip-based pattern can outperform it when $r_c = r_s$ [11]. In 2006, the asymptotic optimality of strip-based patterns that achieve full coverage and 1- and 2-connectivity was proved in for all ranges of r_c/r_s [2]. In 2008, the asymptotically optimal pattern that achieve full coverage and 4-connectivity for $r_c/r_s > \sqrt{2}$ was proposed and proved to be optimal [4]. In [3], a complete set of deployment patterns for all ranges of r_c/r_s that achieve full-coverage and k-connectivity ($k \leq 6$) was proposed. In this set of patterns, those for 3- and 5-connectivity were proved to be optimal for $r_c/r_s \geq 1$ among *regular patterns* (the definition

978-1-4244-5837-0/10/$26.00 ©2010 IEEE

This full text paper was peer reviewed at the direction of IEEE Communications Society subject matter experts for publication in the IEEE INFOCOM 2010 proceedings
This paper was presented as part of the main Technical Program at IEEE INFOCOM 2010.

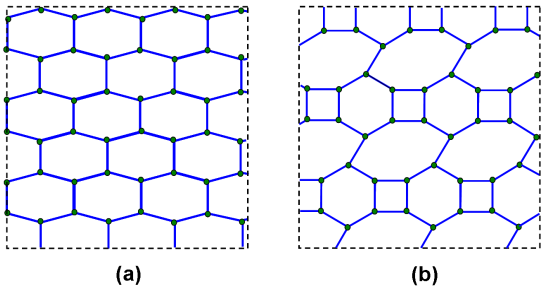

Fig. 2. Mutation in the patterns that achieve full coverage and 3-connectivity when $r_c/r_s = 1.0459$. (a) Hexagon based pattern evolution trend that was believed for all range of r_c/r_s. (b) The hexagon-based trend stops and is replaced by one that is based on a collection of squares, hexagons and octagons.

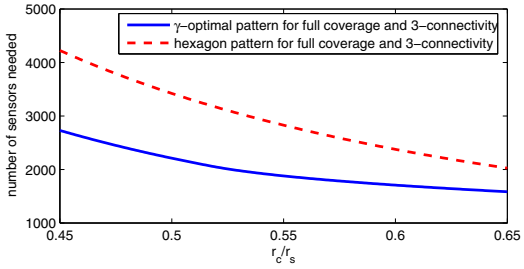

Fig. 3. Number of nodes needed by our new patterns and hexagon pattern for various values of r_c/r_s, when sensors each with $r_s = 30$ m are deployed over a 1,000 m $\times$ 1,000 m region.

of *regular pattern* is given in Section II). Optimality is only conjectured for patterns that achieve 3- and 5-connectivity when $r_c/r_s < 1$, that achieve 4-connectivity when $r_c/r_s \leq \sqrt{2}$, and that achieve 6-connectivity when $r_c/r_s \leq \sqrt{3}$. Recently, the pattern that achieves 6-connectivity when $r_c/r_s \leq \sqrt{3}$ was provided and its optimality among regular deployments was proved in [5]. In this paper, we also focus on regular patterns.

B. Our Contributions

We have conducted further study that aims to prove the aforementioned conjectures. However, we discover the smooth pattern evolution trends are surprisingly broken by a mutation phenomenon that disproves previous conjectures. We highlight our contributions in this paper as follows.

– *Proved New Optimal Patterns.* In this paper, we propose new patterns for full coverage and 3-, 4- and 5-connectivity. We prove their optimality among regular patterns that achieve 3- and 5-connectivity when $r_c/r_s < 1$, and that achieve 4-connectivity when $r_c/r_s \leq \sqrt{2}$. As illustrated in Fig. 1, with our work, the deployment patterns with proved optimality among regular patterns for all ranges of r_c/r_s to achieve full coverage and k-connectivity ($k \leq 6$) is complete.

– *Pattern Mutation.* We discover a surprising pattern mutation phenomenon in pattern evolution as r_c/r_s continuously changes. *Pattern mutation* means that the continuous trend of pattern evolution suddenly stops at a certain value of r_c/r_s and a new pattern evolution trend appears. Fig. 2 presents an example of mutation that happens in the patterns to achieve full coverage and 3-connectivity when $r_c/r_s = 1.0459$. This newly discovered phenomenon contradicts the conjecture made in [3] that states that there exists a universal hexagon-based pattern going through pattern evolution for all ranges of r_c/r_s.

– *Practical Considerations.* We notice that it can be inconvenient to obtain the positions of sensor nodes in some new patterns, which can hamper deployment in practice. From the study on pattern mutation, we design practical patterns that can balance efficiency in terms of the number of required sensor nodes and deployment convenience. The optimality proofs in this paper are based on the disc models that are also adopted by [2], [3], [11], [13], [14], etc. As we know, to build theoretical foundations, abstraction is inevitable. However, it is also important to study patterns under more practical models. In the paper, we also study our proposed patterns under several practical considerations.

C. Significance

Our work has both theoretical and practical significance. To the best of our knowledge, no literature establishes fundamental principles that consider both coverage and connectivity requirements in geometry. This paper and other works [2]–[4] have developed approaches to find some solutions when such foundations are missing. Meanwhile, our discovery of pattern mutation sheds insights on exploration of other fundamental issues. In biology, *mutation* that gives rise to changes in a gene DNA sequence sometimes reflects changing environmental factors, whereas in optimal pattern study, we believe mutation also occurs because the "environment," i.e., the coverage and connectivity factors, changes beyond a certain threshold. Such a phenomenon piques our interest and necessitates increased rigor when studying the multiple covering problem in 2D, the covering problem in 3D space, etc. Aside from pure theoretical contributions, our results are important for several reasons. First, sensor nodes are still not cheap enough. Except for low-end ultrasonic sensors, most sensors usually cost \$100–\$300 apiece. Deploying the minimum number of nodes is important for economic reasons. As shown in Fig. 3, when the XSM platform to detect an All Terrain Vehicle is considered where $r_c/r_s = 0.545$, our new pattern can save 34% of the required sensor nodes compared with the hexagon pattern that is conjectured to be optimal in [3] for 3-connectivity. Second, it is now possible to precisely compute the deployment efficiency of some regular patterns that may be used in practice for deployment convenience. Third, when heuristic algorithms are developed for topology control (i.e., determining a sleep-wakeup schedule for nodes that preserves coverage and/or connectivity), it is possible to compute a precise bound on their performance compared with optimal performance. When developing these algorithms, the insights from the optimal deployment pattern proposed in this paper can be used to improve their performance.

Paper Organization We present system models, definitions, and notations in Section II. In Section III, we introduce the new patterns and the mutation phenomenon. Numerical results are also presented. In Section IV, we prove the asymptotic optimality of these patterns. Practical considerations are discussed in Section V. We conclude in Section VI.

This full text paper was peer reviewed at the direction of IEEE Communications Society subject matter experts for publication in the IEEE INFOCOM 2010 proceedings
This paper was presented as part of the main Technical Program at IEEE INFOCOM 2010.

II. Preliminaries

In our optimal pattern study, we use the disc model for sensing and communication. Each sensor is capable of detecting points only within distance r_s and communicating with other sensors within distance r_c. The disc model for both sensing and communication that provides a useful abstraction from the real world has been widely adopted, e.g., in [2], [4], [11], [13], [14]. We will discuss practical considerations in Section V.

We study the asymptotical optimality of deployment patterns, that is, we consider a relatively large area compared with the sensing and communication ranges. The boundary effect is not important here and can be ignored. We study homogeneous wireless sensor networks where all sensor nodes are identical in terms of sensing and communication capabilities.

In this paper, we use some key definitions in [3] as follows.

Definition 2.1: Communication Graph: A communication graph, denoted by $G_c = (V_c, E_c)$, is a graph that is subject to the following conditions: 1) the elements of its vertex set V are sensors, and 2) the elements of its edge set E are straight line segments connecting all pairs of vertices whose Euclidean distance is no larger than r_c.

Definition 2.2: Deployment Graph: A deployment graph, denoted by $G = (V, E)$, is a planar subgraph of G_c with $V = V_c$ and $E \subseteq E_c$.

There exists a communication graph, G_c, for any given sensor deployment, from which we can obtain multiple deployment graphs. We write $G_k = (V_k, E_k)$ to denote a deployment graph that achieves k-connectivity.

Definition 2.3: Direct Neighbor: In a deployment graph $G = (V, E)$, if there is an edge between two vertices x and y, then x and y are direct neighbors of each other.

Definition 2.4: Angular Distance: The angular distance between two vertices x and y as measured from a given vertex z is the size of the angle $\angle xzy$.[1]

If a vertex x has k_x direct neighbors, then we say that the degree of x in G is k_x. We denote its k_x neighbors by $n_1, n_2, \cdots, n_{k_x}$ in some order. We further denote the angular distance measured from x between n_1 and n_2 by α_{1_x}, between n_2 and n_3 by α_{2_x}, $\cdots$, between n_{k_x-1} and n_{k_x} by α_{k_x-1} and between n_{k_x} and n_1 by α_{k_x}. Now, we are ready to introduce the definition of regular deployment.

Definition 2.5: Regular Deployment: A sensor deployment is called regular if it has a deployment graph G where for any two vertices x and y in G , $k_x = k_y$ and $\alpha_{1_x} = \alpha_{1_y}, \alpha_{2_x} = \alpha_{2_y}, \cdots, \alpha_{k_x} = \alpha_{k_y}$ following the same order.

Definition 2.6: Deployment Polygon: A polygon (i.e., a simple cycle) in a deployment graph is called a deployment polygon.

Definition 2.7: Atomic Deployment Polygon: An atomic deployment polygon, denoted by P^a, is a deployment polygon that contains no vertex or edge in its enclosed region.

[1]In this paper, we give all angles in degrees. We represent θ° by θ for simplicity, e.g., we use 90 to represent 90°, i.e., $\pi/2$.

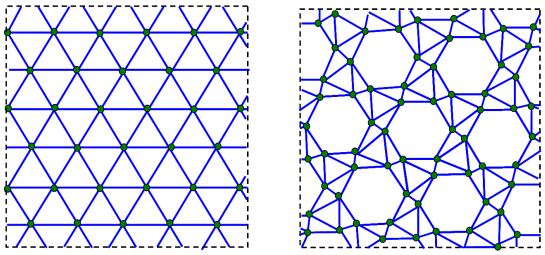

Fig. 4. Solid dots denote sensors. Solid lines denote the communication links established. (a) A deployment graph, G_3, generated by a regular deployment. It can be represented by $\{3.3.3.3.3.3\}$. P^as are triangles. (b) G_5 $\{6.3^*(80).3^*(80).3.3^*(20)\}$. P^as are hexagons and triangles.

Definition 2.8: γ-Optimal Pattern: A regular deployment pattern is called γ-optimal if it needs the minimum number of sensors to achieve a given coverage and connectivity requirement, among all regular patterns.

An atomic deployment polygon does not "contain" any other deployment polygons. We denote a regular P^a by P^a_r and an α-sided P^a by $P^a(\alpha)$. We denote a γ-optimal pattern that achieves full coverage and k-connectivity by $\mathcal{P}^o_k$.

In this paper, we use *vertex configuration* to represent deployment graphs. It is given in geometry as a sequence of numbers representing the information of the faces going around the vertex. A regular α-edged polygon is denoted by α; an irregular α-edged polygon is denoted by α^*; if the faces going around a vertex are a regular α-edged polygon, an irregular β-edged polygon, and a regular polygon with γ sides, then the configuration of this vertex is $\{\alpha.\beta^*.\gamma\}$. We often add angle information to vertex configuration. By $\alpha^*(\theta)$, it indicates the angle at this vertex of an irregular α-edged polygon is θ. Fig. 4 illustrates two deployment graphs generated by regular deployments, which can be presented by $\{3.3.3.3.3.3\}$ and $\{6.3^*(80).3^*(80).3.3^*(20)\}$, respectively.

Studying optimality among regular patterns sheds insights on exploring globally optimal patterns. For examples, all known globally optimal deployment patterns are in fact regular, which include the triangular pattern [12], strip-based pattern [2], and the 4-connectivity patterns proposed in [4]. Regularity also has strong practical indications in homogeneous WSNs. However, the exploration (design and proof) of optimal patterns is not trivial, even among regular ones.

III. Pattern Mutation

In this section, we present optimal patterns for all range of r_c/r_s and mutation phenomena for 3-, 4- and 5-connectivity.

A. Optimal Patterns for 3-Connectivity

Fig. 5 shows how optimal patterns that achieve full coverage and 3-connectivity evolve as r_c/r_s decreases. We present the pattern description for $\mathcal{P}^o_3$ as follows. The distance between two connected sensors is denoted by d.

- $\sqrt{3} \leq r_c/r_s$: $\{6^*(60).6^*(120).6^*(180)\}$, shown in Fig. 5(a). $d = \sqrt{3}r_s$.

This full text paper was peer reviewed at the direction of IEEE Communications Society subject matter experts for publication in the IEEE INFOCOM 2010 proceedings
This paper was presented as part of the main Technical Program at IEEE INFOCOM 2010.

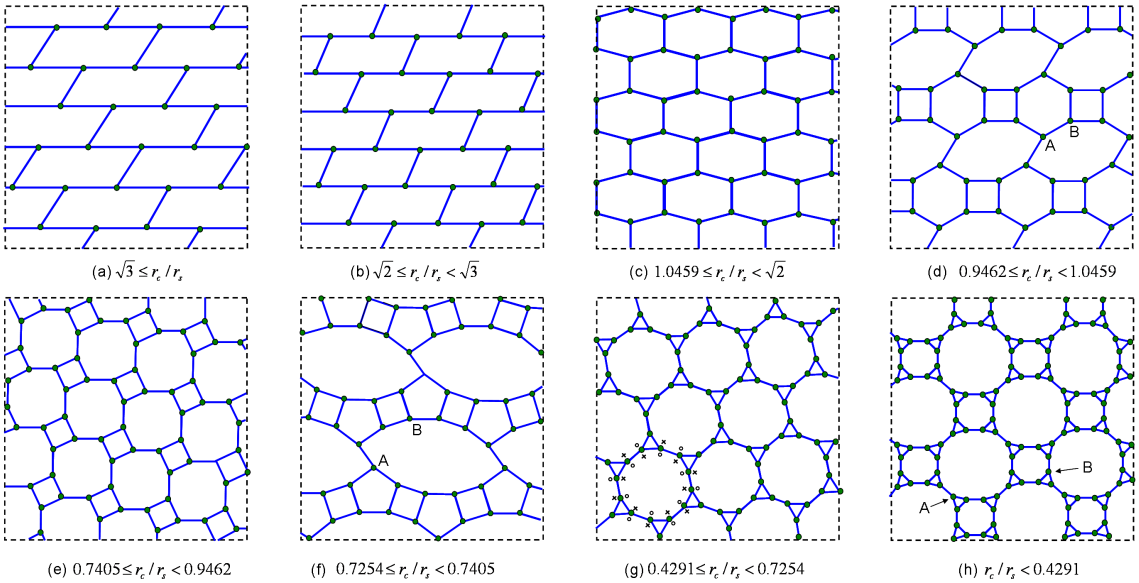

(a) $\sqrt{3} \le r_c/r_s$ (b) $\sqrt{2} \le r_c/r_s < \sqrt{3}$ (c) $1.0459 \le r_c/r_s < \sqrt{2}$ (d) $0.9462 \le r_c/r_s < 1.0459$

(e) $0.7405 \le r_c/r_s < 0.9462$ (f) $0.7254 \le r_c/r_s < 0.7405$ (g) $0.4291 \le r_c/r_s < 0.7254$ (h) $r_c/r_s < 0.4291$

Fig. 5. Optimal deployment patterns to achieve full coverage and 3-connectivity for a full range of r_c/r_s.

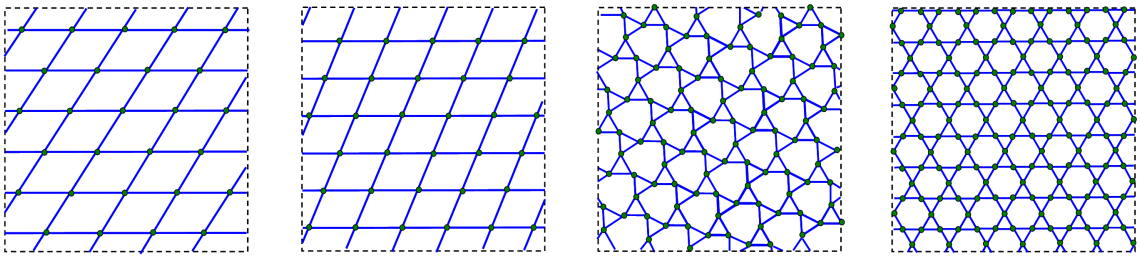

(a) $\sqrt{3} \le r_c/r_s$ (b) $1.3903 \le r_c/r_s < \sqrt{3}$ (c) $1 \le r_c/r_s < 1.3903$ (d) $r_c/r_s < 1$

Fig. 6. Optimal deployment patterns to achieve full coverage and 4-connectivity for a full range of r_c/r_s.

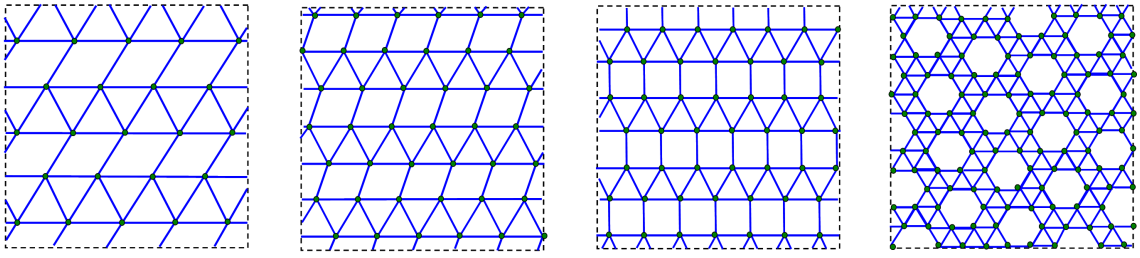

(a) $\sqrt{3} \le r_c/r_s$ (b) $\sqrt{2} \le r_c/r_s < \sqrt{3}$ (c) $1.0406 \le r_c/r_s < \sqrt{2}$ (d) $r_c/r_s < 1.0406$

Fig. 7. Optimal deployment patterns to achieve full coverage and 5-connectivity for a full range of r_c/r_s.

- $\sqrt{2} \le r_c/r_s < \sqrt{3}$: $\{6^*(\theta_1).6^*(\theta_2).6^*(180)\}$, shown in Fig. 5(b), where $\theta_1 = 2\arccos\frac{2r_c}{r_s}$, $\theta_2 = 180 - \theta_1$. $d = r_c$.
- $1.0459 \le r_c/r_s < \sqrt{2}$: $\{6^*(\theta_1).6^*(\theta_2).6^*(\theta_2)\}$, shown in Fig. 5(c), where $\theta_1 = 4\arcsin\frac{r_s}{2r_c}$ and $\theta_2 = (360 - \theta_1)/2$. $d = r_c$.
- $0.9462 \le r_c/r_s < 1.0459$: $\{6.8^*(90).8^*(150)\}$ (e.g., the sensor at position A) and $\{6.4.8^*(150)\}$ (e.g., the sensor at position B), shown in Fig. 5(d). $d = r_c$.
- $0.7405 \le r_c/r_s < 0.9462$: $\{4.8^*(\theta_1).8^*(\theta_2)\}$, shown in Fig. 5(e). When $0.7655 \le r_c/r_s < 0.9462$, $\theta_1 = 2\arcsin\frac{\sqrt{2}r_s}{2r_c}$, $\theta_2 = 270 - \theta_1$, $d = 0.7655r_s$. When $0.7405 \le r_c/r_s < 0.7655$, $\theta_1 = \theta_2 = 135$ (i.e., $\{4.8.8\}$), $d = r_c$.
- $0.7254 \le r_c/r_s < 0.7405$: $\{12^*(90).12^*(162).5\}$ (e.g., the sensor at position A) and $\{4.5.12^*(162)\}$ (e.g., the sensor at position B), shown in Fig. 5(f). When $0.7254 \le r_c/r_s < 0.7403$, $d = r_c$. When $0.7403 \le r_c/r_s < 0.7405$, $d = 0.7403r_s$.
- $0.4291 \le r_c/r_s < 0.7254$: $\{12^*(\theta_1).12^*(\theta_2).3\}$, shown in Fig. 5(g) where θ_1 and θ_2 are denoted by "$\circ$" and "$\times$", respectively. When $0.5176 \le r_c/r_s < 0.7254$, $\theta_1 = 2\arcsin\frac{r_s}{2r_c}$, $\theta_2 = 300 - \theta_1$. When $0.4291 \le r_c/r_s < 0.5176$, $\theta_1 = \theta_2 = 150$ (i.e., $\{3.12.12\}$). $d = r_c$.

This full text paper was peer reviewed at the direction of IEEE Communications Society subject matter experts for publication in the IEEE INFOCOM 2010 proceedings
This paper was presented as part of the main Technical Program at IEEE INFOCOM 2010.

– $r_c/r_s < 0.4291 : \{3.16^*(135).16^*(165)\}$ (e.g., the sensor at position A) and $\{3.8.16^*(165)\}$ (e.g., the sensor at position B), shown in Fig. 5(h). When $0.4118 \leq r_c/r_s < 0.4291$, $d = 0.4118r_s$. When $r_c/r_s < 0.4118$, $d = r_c$.

Recall the notation of vertex configuration in Section II. $\{6^*(60).6^*(120).6^*(180)\}$ when $\sqrt{3} \leq r_c/r_s$ (shown in Fig. 5(a)) suggests that each node is shared by three irregular hexagons in this pattern. Three inner angles at this node from these hexagons are 60, 120 and 180, respectively. When $0.9462 \leq r_c/r_s < 1.0459$ (shown in Fig. 5(d)), $\{6.8^*(90).8^*(150)\}$ and $\{6.4.8^*(150)\}$ suggest that there are two types of nodes. Each node of the first type is shared by one regular hexagon and two irregular octagons, while each of the second type is shared by one regular hexagon, one square and one irregular octagon.

Mutation occurs when some trend of pattern changes is stopped by another pattern. As shown in Fig. 5(a)–(c), when $r_c/r_s \geq 1.0459$, there exists a universal hexagon-based pattern that provides the elementary unit for pattern evolution as r_c/r_s decreases. The trend of such variation is to enlarge the area of the hexagon with decreasing r_c and while maintaining full coverage at the same time. This trend was conjectured in [3] to continue for all ranges of r_c/r_s. However, our new patterns show that mutation occurs at the point of $r_c/r_s = 1.0459$. The aforementioned trend is stopped by a new pattern shown in Fig. 5(d). In this new pattern, the hexagon-based trend breaks and is replaced by one that is based on a collection of squares, hexagons and octagons. Such mutation happens 5 times in the evolution of patterns that achieve full coverage and 3-connectivity. The mutation points are 1.0459, 0.9462, 0.7405, 0.7254 and 0.4291.

B. Optimal Patterns for 4- and 5-Connectivity

Fig. 6 shows how the optimal patterns that achieve full coverage and 4-connectivity evolve as r_c/r_s decreases. We present the pattern description for $\mathcal{P}_4^o$ as follows.

– $\sqrt{3} \leq r_c/r_s : \{4^*(60).4^*(120).4^*(60).4^*(120)\}$, shown in Fig. 6(a). $d = \sqrt{3}r_s$.
– $1.3903 \leq r_c/r_s < \sqrt{3} : \{4^*(\theta_1).4^*(\theta_2).4^*(\theta_1).4^*(\theta_2)\}$, shown in Fig. 6(b). When $\sqrt{2} \leq r_c/r_s < \sqrt{3}$, $\theta_1 = 2\arccos\frac{2r_c}{r_s}$, $\theta_2 = 180 - \theta_1$. When $1.3903 \leq r_c/r_s < \sqrt{2}$, $\theta_1 = \theta_2 = 90$ (i.e., $\{4.4.4.4\}$). $d = r_c$.
– $1 \leq r_c/r_s < 1.3903 : \{3.6^*(\theta_1).3.6^*(\theta_2)\}$, shown in Fig. 6(c), where $\theta_1 = 2\arcsin\frac{\sqrt{3}r_s}{r_c}$, $\theta_2 = 240 - \theta_1$. $d = r_c$.
– $r_c/r_s < 1 : \{6.3.6.3\}$, shown in Fig. 6(d). $d = r_c$.

In these patterns shown in Fig. 6, there exists one mutation point at $r_c/r_s = 1.3903$.

Fig. 7 shows how the optimal patterns that achieve full coverage and 5-connectivity evolve as r_c/r_s decreases. We present pattern description for $\mathcal{P}_5^o$ as follows.

– $\sqrt{3} \leq r_c/r_s : \{4^*(60).4^*(120).3.3.3\}$, shown in Fig. 7(a). $d = \sqrt{3}r_s$.
– $\sqrt{2} \leq r_c/r_s < \sqrt{3} : \{4^*(\theta_1).4^*(\theta_2).3.3.3\}$, shown in Fig. 7(b), where $\theta_1 = 2\arccos\frac{2r_c}{r_s}$, $\theta_2 = 180 - \theta_1$. $d = r_c$.

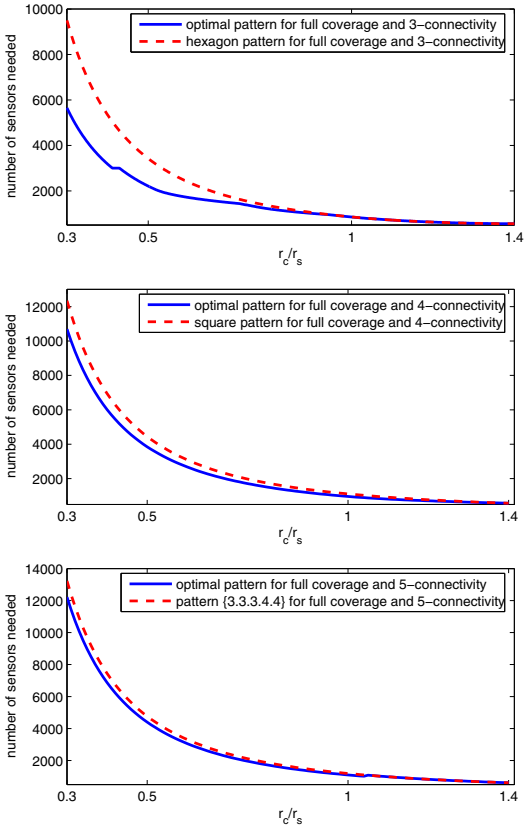

Fig. 8. Nodes needed in $\mathcal{P}_3^o$, $\mathcal{P}_4^o$, and $\mathcal{P}_5^o$ when compared with the conjectured-optimal patterns in [3], respectively. Sensors each with $r_s = 30$ m are deployed over a $1{,}000^2$ m^2 region. r_c is from $0.3r_s$ to $\sqrt{2}r_s$.

– $1.0406 \leq r_c/r_s < \sqrt{2} : \{4.4.3.3.3\}$, shown in Fig. 7(c). $d = r_c$.
– $r_c/r_s < 1.0406 : \{6.3.3.3.3\}$, shown in Fig. 7(d). $d = r_c$.

In these patterns shown in Fig. 7, there also exists only one mutation point at $r_c/r_s = 1.0406$.

C. Numerical Results

Fig. 8 illustrates how many sensor nodes can be saved by our γ-optimal patterns when compared with the conjectured optimal patterns in [3]. Sensors each with $r_s = 30$ m are deployed over a $1,000^2$ m^2 region. r_c is from $0.2r_s$ to $\sqrt{2}r_s$.

– For 3-connectivity, our pattern can save many required nodes compared with the conjectured optimal hexagon-based pattern. When $r_c/r_s = 0.3$, it can save 40.5% of the required nodes. When $r_c/r_s = 0.5$, it can save 35.4% of the required nodes.
– For 4-connectivity, our pattern can save more than 13% of the required nodes compared with the conjectured optimal square-based pattern when $r_c/r_s \leq 1$.
– For 5-connectivity, our pattern can save around 8% of the required nodes compared with the conjectured optimal pattern $\{3.3.3.4.4\}$ when $r_c/r_s \leq 1$.

This full text paper was peer reviewed at the direction of IEEE Communications Society subject matter experts for publication in the IEEE INFOCOM 2010 proceedings
This paper was presented as part of the main Technical Program at IEEE INFOCOM 2010.

IV. Optimality Proof

In this section, we provide optimality proofs for the patterns proposed in Section III.

A. Optimality of 3-Connectivity Patterns

Theorem 4.1: Patterns as shown in Fig. 5 are γ-optimal to achieve full coverage and 3-connectivity.

We begin by introducing the roadmap of our proof. The optimality proof for 3-connectivity patterns consists of two major steps. *In the first step*, we find all possible regular patterns that can satisfy full coverage and connectivity requirements. In this step, we take advantage of regular deployments' macroscopic properties to divide the search space into smaller spaces. *In the second step*, we compare the patterns obtained from the first step for ranges of r_c/r_s to obtain optimality. Comparison among different patterns is based on the average area that each sensor covers in these patterns. A basic deployment graph with a k-connectivity regular pattern consists of m types of p^αs. If the measure and the edge number of each polygon of the ith type is S_i and e_i respectively, and the ratio of the number of polygons in each type is $r_1, \cdots, r_m$, then the average area that each sensor covers is $S = k\sum_{i=1}^{m} r_i S_i/(\sum_{i=1}^{m} r_i e_i)$. The pattern is optimal if and only if S has the maximal value.

To find out all possible regular patterns, the following Lemma 4.1 establishes an important foundation.

Lemma 4.1: In a regular deployment with k-connectivity ($k = 3, 4, 5$) consisting of n sensors, let ω_k denote the average edge number of atomic deployment polygons. Then $\lim_{n\to\infty} \omega_3 = 6$, $\lim_{n\to\infty} \omega_4 = 4$, and $\lim_{n\to\infty} \omega_5 = 10/3$.

Proof: Any planar deployment graph G_k with $k > 2$ can be considered as a non-overlapped tiling of a set of deployment polygons. Let the number of deployment polygons in G_k be denoted by N_P, the degree of the ith vertex by μ_i.

Then from the Euler relationship, we have $|V_k| - |E_k| + N_P = 1$. Since each edge has two vertices, $\sum_{i=1}^{|V_k|} \mu_i = 2|E_k|$. Replacing it into the Euler relationship, we obtain $\sum_{i=1}^{|V_k|}(\mu_i - 2) + 2 = 2N_p$. Hence the average edge number of atomic deployment polygons in G_k is

$$\omega = \textstyle\sum_{i=1}^{|V_k|} \mu_i/N_p = (2\sum_{i=1}^{|V_k|} \mu_i)/(\sum_{i=1}^{|V_k|}(\mu_i - 2) + 2).$$

By substituting $|V_k| = n$ and $\mu_i = m$ in the above equation and taking the limit, we obtain the Lemma. ■

Lemma 4.1 shows the average number of edges of P^as are asymptotically bounded. It suggests the polygon types in a regular deployment cannot be random. The following Lemma 4.2 presents all the possible regular patterns.

Lemma 4.2: Among the patterns consisting of equilateral P^as, all possible regular patterns that can satisfy full coverage and 3-connectivity requirements, besides those appear in Fig. 5, are $\{12.4.6\}$ and $\{16^*(160).3.10^*(140)\}$ (or $\{16^*(160).3.16^*(140)\}$, $\{10^*(160).3.10^*(140)\}$) as shown in Fig. 9.

The proof of Lemma 4.2 is very long and due to space limitations, we present the proof in [6].

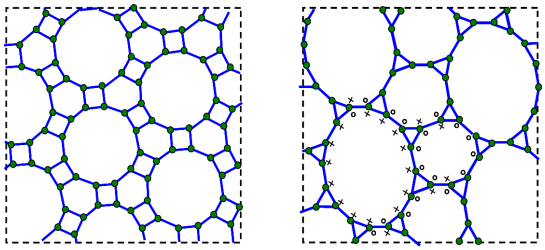

Fig. 9. (a) The $\{12.4.6\}$ pattern. (b) There are three types of vertex configurations in this pattern $\{16^*(160).3.10^*(140)\}$ or $\{16^*(160).3.16^*(140)\}$ or $\{10^*(160).3.10^*(140)\}$. The 160 angles are denoted by "×" and the 140 angles are denoted by "○".

To prove Theorem 4.1, we also need several useful conclusions that have been published. From [3], to search for optimal patterns, we only need to consider the patterns consisting of equilateral P^as. Also, it has been proved in Theorems 4.1 and 4.5 of [3] that any regular deployment can be considered as a set of atomic deployment polygons covering the same area. Now we can prove Theorem 4.1.

Proof: (1) It was proved in the proof of Theorem 4.1 of [5] that the Theorem is true for the cases where $r_c/r_s \geq 1.0459$[2], and when $r_c/r_s < 1.0459$, the average area that each sensor covers in Fig. 5(d) is bigger than that in Fig. 5(c). Also, it was proved there that the average area that each sensor of covers in Fig. 5(d) is $(7+5\sqrt{3})r_c^2/12$ when the edge length of polygons is $r_c \leq r_s$.

(2) We consider the pattern $\{4.8^*(\theta_1).8^*(\theta_2)\}$. We consider the pattern $\{4.8.8\}$ first. To achieve full coverage, the sensors placed in the regular octagons' vertices should cover the octagons' area completely, and hence the distance between the vertexes and the center of a octagon should not be greater than r_s. This is the case when the edge length r_c of octagons is not greater than $2\cos 67.5 r_s$ and then the average area each sensor covers is $(3+2\sqrt{2})r_c^2/4 = 1.4571 r_c^2$.

When $r_c/r_s > 2\cos 67.5 = \sqrt{2-\sqrt{2}} = 0.7655$, one way to achieve full coverage is by transforming the edge r_c into $\alpha r_c (0 < \alpha < 1)$ such that $\alpha r_c/r_s = 2\cos 67.5$ and then the average area each sensor covers is $\alpha^2(3+2\sqrt{2})r_c^2/4$. Another way to achieve full coverage is by keeping the edge r_c unchanged while changing the regular octagons into octagons with two types of inner angles such that the sum of these angles is 270. Denote the smaller inner angles of octagons by $2A$ $(45 < A < 67.5)$. When the distance between a vertex with a larger inner angle and the center of a octagon is not greater than r_s, the sensors placed in the octagons' vertices cover the octagons's area completely. When this distance is r_s, $A = \arcsin(\sqrt{2}r_s)/(2r_c)$ and the area of an octagon is $S_8 = 2r_s^2 + 4r_c^2 \sin A \cos A$. As $\alpha r_c/r_s = 2\cos 67.5 = \sqrt{2-\sqrt{2}}$, we find that $S_8 = [(2+\sqrt{2})\alpha^2 + 2\sin 2A]r_c^2$. Hence the average area that each sensor covers is $[(2+\sqrt{2})\alpha^2 + 2\sin 2A + 1]r_c^2/4$. As $0 < \alpha < 1$ and $45 < A < 67.5$, this area is greater than $\alpha^2(3+2\sqrt{2})r_c^2/4$, which means that the average area

[2]We keep the first four digits after the decimal point in the proofs.

This full text paper was peer reviewed at the direction of IEEE Communications Society subject matter experts for publication in the IEEE INFOCOM 2010 proceedings
This paper was presented as part of the main Technical Program at IEEE INFOCOM 2010.

that each sensor covers in the latter case is larger than that in the former case. To make this area larger than the average area that each sensor covers in the pattern considered in Fig. 5(d), we need $[(2+\sqrt{2})\alpha^2+2\sin 2A+1]/4 \geq (7+5\sqrt{3})/12$. Since $\sin A = \sqrt{2}r_s/(2r_c)$ and $\alpha r_c/r_s = 2\cos 67.5 = \sqrt{2-\sqrt{2}}$, we have $\sin A = \alpha/\sqrt{4-2\sqrt{2}}$. Hence, from the above inequality we obtain that $\alpha = 0.8089$. It follows that $r_c/r_s = 2\cos 67.5/\alpha \leq 0.9462$.

(3) By an argument similar to that of (2), we can prove that when $r_c/r_s \leq 0.7405$, the average area that each sensor covers in the pattern considered in Fig. 5(f) is larger than that considered in Fig. 5(e); when $r_c/r_s \leq 0.7254$, the average area each sensor covers in the pattern considered in Fig. 5(g) is larger than that considered in Fig. 5(f); and when $r_c/r_s \leq 0.4291$, the average area each sensor covers in the pattern considered in Fig. 5(h) is larger than that considered in Fig. 5(g). We omit the detailed proof because of space limitations. The details are provided in [6].

(4) We prove neither $\{12.4.6\}$ nor $\{16^*(160).\ 3.10^*(140)\}$ (or $\{16^*(160).3.16^*(140)\}$, or $\{10^*(160).3.10^*(140)\}$) can be optimal pattern. We compare the $\{12.4.6\}$ pattern with the pattern considered in Fig. 5(g). To achieve full coverage in the $\{12.4.6\}$ pattern, the distance between a vertex and the center of the dodecagon is not greater than r_s, which occurs only when the edge length r_c of polygons is not greater than $\sqrt{2-\sqrt{3}}r_s = 0.5176r_s$. Then the pattern considered in Fig. 5(g) should be $\{12.12.3\}$. Since in the $\{12.4.6\}$ pattern, the ratio of dodecagons, hexagons and squares is 1:2:3, the average area that each sensor covers is $(3\tan 75+3\tan 60+3)r_c^2/12 = 1.6160r_c^2$; while in pattern $\{12.12.3\}$, the ratio of dodecagons and triangles is 1:2, the average area that each sensor covers is $(3\tan 75 + \tan 60/2)r_c^2/6 = 2.0103r_c^2$. Since the latter one is bigger than the former one, the $\{12.4.6\}$ pattern is not optimal. Similarly, compare pattern $\{16^*(160).3.10^*(140)\}$ (or $\{16^*(160).3.16^*(140)\}$, or $\{10^*(160).3.10^*(140)\}$) with the pattern considered in Fig. 5(g), we can prove this pattern is not optimal neither.

By Lemma 4.2 and steps (1)–(4) above, we have proved Theorem 4.1. ■

Remarks: (1) Pattern mutation derives from the fact that the average area that each sensor covers in different patterns changes in different speed as r_c/r_s varies, as illustrated in our proof. (2) In [3], we ignored the patterns considered in Fig. 5(d) and declared that the hexagon pattern is optimal when $r_c/r_s \geq 1$. This error was corrected in [5]. (3) In the example of [1] which we mentioned in Section I, $r_c/r_s = 0.545$ and the optimal pattern in this case is $\{12^*(133).12^*(167).3\}$. When the edge length of polygons is r_c, the average area each sensor covers is $1.9672r_c^2$ in this pattern, while the average area each sensor covers is only $1.2990r_c^2$ in the hexagon pattern. That verifies our new pattern can save around 34% of sensor nodes compared with the hexagon pattern.

B. Optimality of 4- and 5-Connectivity Patterns

Theorem 4.2: Patterns as shown in Fig. 6 are γ-optimal to achieve full coverage and 4-connectivity.

Proof: By Lemma 4.1, we find that the average edge number of all atomic deployment polygons is 4. We first consider the case where all P^as have 4 edges. When $1 < r_c/r_s < \sqrt{2}$, the maximum area occurs when P^as are squares. As r_c/r_s further increases, the maximum area occurs as P^as are rhombuses. It was proved in [4], the pattern shown in Fig. 6(a) and (b) are optimal when $r_c/r_s > \sqrt{2}$.

We then consider the case where there are P^as with n edges ($n > 4$). By our assumption, each n-sided P^a must be paired with $n-4$ triangles. When $n > 6$, $3(n-4) > n$. Hence, among the four angles that share one vertex, there must be two 60 angles and the other two with average 120. This implies that the polygon consisting of these two angles whose average is not greater than 120, which is a contradiction for $n > 6$. Hence, we only need to consider $n = 5$ and $n = 6$.

We then first consider $n = 5$. If an equilateral pentagon is irregular, it must have at least three types of inner angles, among which there exist three angles whose sum is larger than 324. This is impossible, since there will be no 60 angles. If a pentagon is regular, then among the four angles that share one vertex, there is at least one 60 angle, one 108 angle. The left two angles cannot be both 60 nor one 60 and one 108. So there must be another type of polygon whose edge number is larger than 3. Since it has been shown this type of polygon can only be a hexagon and the average of a hexagon's inner angles is 120, it is impossible. Hence, only $n = 6$ should be considered.

When $n = 6$, among the four angles that share one vertex, there are two 60 angles, and the other two have average 120. The pattern is $\{6.3.6.3\}$. When $r_c \leq r_s$, if the hexagon is regular with edge length r_c, then the sensors located in the hexgaon's vertices can cover its area completely. Since the ratio of triangles to hexagons is 2:1 in this pattern, the average area that each sensor covers is $\frac{2\sqrt{3}}{3}r_c^2 = 1.1547r_c^2$. When $r_c > r_s$, the first way to achieve full coverage is by transforming the edge r_c into kr_c $(0 < k < 1)$ such that $kr_c = r_s$. In this case, the average area that each sensor covers is $\frac{2\sqrt{3}}{3}k^2r_c^2$. The second way to achieve full coverage is by changing the inner angles of regular hexagons into two types of inner angles such that the sum of two types of inner angles is 240 while keeping the edge r_c unchanged. This pattern is $\{3.6^*(\theta_1).3.6^*(\theta_2)\}$, where $\theta_1 = 2\arcsin\frac{\sqrt{3}r_s}{r_c}$, $\theta_2 = 240-\theta_1$. With arguments that are similar to that in the second step in the proof for Theorem 4.1, we are able to prove the average area that each sensor covers in the second way is larger than that in the first way and larger than that in the rhombus pattern when $r_c/r_s < 1.3903$. ■

Theorem 4.3: Patterns as shown in Fig. 7 are γ-optimal to achieve full coverage and 5-connectivity.

The proof for Theorem 4.3 is similar to that for Theorem 4.2. We give the proof in [6].

V. Practical Considerations

A. Pattern Deployment

In this section, we show how to deploy sensors following the above optimal patterns and present some practical deployment

This full text paper was peer reviewed at the direction of IEEE Communications Society subject matter experts for publication in the IEEE INFOCOM 2010 proceedings
This paper was presented as part of the main Technical Program at IEEE INFOCOM 2010.

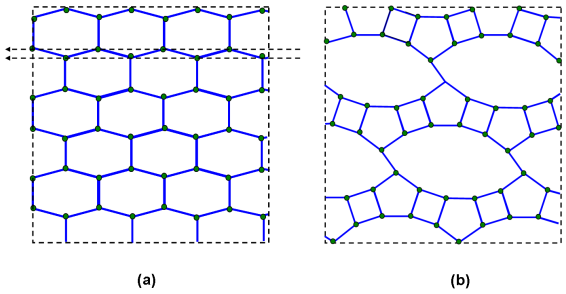

Fig. 10. (a) This pattern can be easily deployed based on the location of sensors in lines and the distance between lines. (b) In this pattern, the number of lines and the positions of sensors (particularly the first sensor) at each line are not easy to obtain.

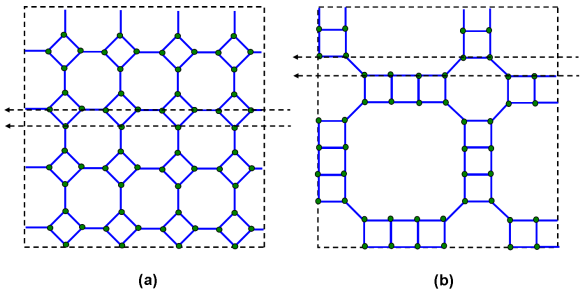

Fig. 11. Patterns we design for full-coverage and 3-connectivity. (a) For $0.6184 \leq r_c/r_s < 0.8089$. (b) For $r_c/r_s < 0.4813$.

patterns designed for the purpose of deployment convenience.

Due to regularity of the proposed patterns, we can deploy sensors along certain lines. We call these lines *deployment lines*. For example, to deploy the pattern shown in Fig. 10(a), we can first deploy sensors along the dashed lines and then repeat this process. More specifically, we have two types of lines in this example according to the sensor node positions along the line. The horizontal positions of each sensor on one line are in the middle of two neighboring sensor nodes on the other line. To deploy such a pattern, we only need to control the locations of sensor nodes in the line (particularly the first sensor) and the distance between lines. Deployment can be facilitated by repeating the process of deploying sensors at multiple lines. However, in some optimal patterns there are several deployment lines and the positions of sensors are not easy to obtain, e.g., the pattern shown in Fig. 10(b). This may hamper such patterns' applications in spite of their optimality.

We learn from pattern mutation that "bubbles" appear when r_c/r_s is small. We then tackle the problem by designing new patterns that can balance deployment convenience and optimality. Fig. 11(a) shows the pattern that we design for $0.6184 \leq r_c/r_s < 0.8089$ for 3-connectivity. In this pattern, when $0.7655 \leq r_c/r_s < 0.8089$, $d = 0.7655r_s$; when $0.6184 \leq r_c/r_s < 0.7655$, $d = r_c$. Fig. 11(b) shows the pattern that we design for $r_c/r_s < 0.4813$. In this pattern, when $0.4531 \leq r_c/r_s < 0.4813$, $d = 0.4531r_s$; when $r_c/r_s < 0.4531$, $d = r_c$. When $0.4813 \leq r_c/r_s < 0.6184$, the pattern that we design is similar to Fig. 11(b) that consists of squares, equilateral octagons and equilateral dodecagons with two squares at each side (in Fig. 11(b) there are three squares

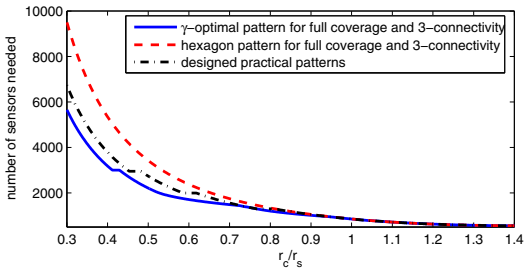

Fig. 12. Number of nodes needed in optimal patterns $\mathcal{P}_3^o$, our designed practical patterns, and the hexagon pattern. Sensors each with $r_s = 30$ m are deployed over a $1,000\ m \times 1,000\ m$ region. r_c varies from $0.3r_s$ to $\sqrt{2}r_s$.

at each side). In this pattern, when $0.5858 \leq r_c/r_s < 0.6184$, $d = 0.5858r_s$; when $0.4813 \leq r_c/r_s < 0.5858$, $d = r_c$. The above ranges are determined by comparing the average area that each sensor covers and the requirement to achieve full coverage. The derivations thereof can be found in [6]. These patterns are easy to deploy. Each pattern has two types of deployment lines. Fig. 12 shows the number of nodes needed with the optimal patterns $\mathcal{P}_3^o$, our designed practical patterns, and the hexagon pattern that was conjectured optimal in [3], respectively. Compared with the hexagon pattern, these patterns can save 16% sensor nodes when $r_c/r_s = 0.6$, around 20% when $r_c/r_s = 0.5$, and around 29.2% when $r_c/r_s = 0.4$.

Interestingly, during the above pattern design procedure that follows what we have learned from the mutation phenomenon, we discover that γ-optimal patterns are not necessarily *globally* optimal. This is an intriguing direction for our future work.

B. Other Practical Considerations

In reality, the sensing range may follow certain statistical models [16], [23]. The disc model can be obtained from these models by first setting a desirable threshold for sensing quality or probability, and then exploiting this threshold to determine the largest possible distance between the sensor and the target. This distance is considered the sensing range r_s. In some cases, the sensing area is non-disc even after a threshold has been set. Cao et al. in [8] suggest the sensing capability roughly follows a Gaussian distribution over different directions. We study by simulation the impact from such sensing irregularity on coverage in our optimal deployment patterns. Due to space limitations, the results are not shown in this paper. From the simulation results, we observe that higher sensing irregularity will result in lower overall coverage and a smaller r_c value can help overcome the decreased coverage shrinking brought by sensing irregularity. These observations can be explained from the view of overlapping areas. The deployment patterns that generate more overlapping area are more tolerant to sensing irregularities. Given each sensor's sensing area, there are naturally two ways to increase overlapping areas in patterns: (1) adopt a smaller communication range such that sensors are closer to each other; (2) adopt deployment patterns that can achieve higher connectivity such that more sensors overlap.

To consider a practical communication model, we use a widely used model suggested by Zuniga and Krishnamachari

in [24]. This model established the function of the distance between the transmitter and the receiver and the communication link quality measured by the *packet reception rate* PRR. At distance d, the PRR can be expressed as $PRR(d) = (1 - \exp(-\frac{P_t - PL(d) - P_n}{2})/2)^{8\ell}$, where P_t is the output power of the transmitter, $PL(d)$ is the path loss at distance d, P_n is the noise floor and ℓ is the frame length. We run simulations for each sensor to establish local 1–6 connectivity, respectively. We consider the connection established when $PRR \geq 0.95$. We let r_c/r_s vary from 0.3–1.8 such that all patterns are covered. We pick the transmission power P_t in the above model to illustrate its impact since it is an adjustable property of a physical device and does not depend on the external environment. For each combination of P_t and an optimal pattern, we run simulations 10,000 times. The probability is then the ratio of the number of times when a link with $PRR \geq 0.95$ can be established to 10,000. Other parameters are from empirical data in [24].

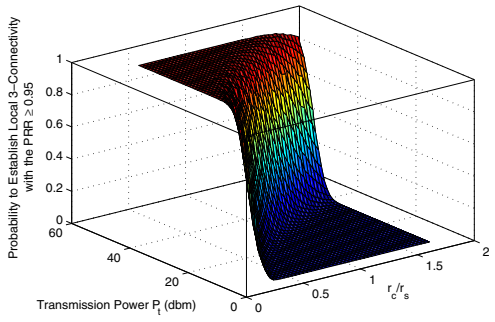

Fig. 13. The probability for a sensor to establish links with PRR ≥ 0.95 to three specific neighbors for different transmission power P_t and distance d. $r_s = 30$ m.

In our results, as the transmission power increases for a given pattern decided by r_c/r_s, we notice that the probability transition from 1 to 0 gets slightly sharper as the connectivity k increases. Due to space limitations, we only show this for 3-connectivity in Fig. 13. The smoothly changing surfaces also illustrate that if we want to ensure local k-connectivity (and hence global k-connectivity) in practice with high probability, the output power P_t should satisfy $1 - P[\mathcal{F}(r_c, r_s, P_t) \geq x]^k \leq \epsilon$, where the function $\mathcal{F}$ calculates the PRR, x denotes a threshold of the PRR above which the link quality is considered acceptable, and ϵ is a small positive number.

In real deployment, we should also consider deployment errors and how to overcome geographical constraints on deployment area. In some cases, hierarchical sensor network architectures are desirable. Providing a fundamental reference, our optimal deployment patterns in this paper are still valuable when these practical issues are considered. Further discussion on these issues is omitted in the paper due to space limitations. Interested reader can refer to [2]–[6] for detailed discussion.

VI. Conclusion

In this paper, we present and study a surprising and interesting pattern mutation phenomenon discovered in our exploration of pattern optimality. This phenomenon contradicts the conjectures presented in a previous work that there exists a universal elemental pattern among optimal pattern evolution and the pattern evolution is continuous. Our work also further completes the exploration of optimal patterns in WSNs. Searching for optimal patterns among all patterns (beyond regular constraints) and proving their optimality are part of our future work. We will also extend our proposed patterns under practical models.

References

[1] A. Arora et al. ExScal: Elements of an Extreme Scale Wireless Sensor Network. In *Proc. of IEEE RTCSA,* 2005.
[2] X. Bai, S. Kumar, D. Xuan, Z. Yun and T. H. Lai. Deploying Wireless Sensors to Achieve Both Coverage and Connectivity. In *Proc. of ACM MobiHoc,* 2006.
[3] X. Bai, D. Xuan, Z. Yun, T. H. Lai and W. Jia. Complete Optimal Deployment Patterns for Full-Coverage and k-Connectivity ($k \leq 6$) Wireless Sensor Networks. In *Proc. of ACM MobiHoc,* 2008.
[4] X. Bai, Z. Yun, D. Xuan, T. H. Lai and W. Jia. Deploying Four-Connectivity And Full-Coverage Wireless Sensor Networks. In *Proc. of IEEE INFOCOM,* 2008.
[5] X. Bai, D. Xuan, Z.Yun, T. Lai, and W. Jia. Complete Optimal Deployment Patterns for Full-Coverage and k-Connectivity ($k \leq 6$) Wireless Sensor Networks. *Technical Report. At* http://www.cse.ohio-state.edu/∼baixia/publications/TR09-1-Complete.pdf.
[6] X. Bai, Z. Yun, D. Xuan, W. Jia and W. Zhao. Pattern Mutation in Wireless Sensor Deployment. *Technical Report.* At *http://www.cse.ohio-state.edu/∼baixia/publications/TR09-2-Mutation.pdf.*
[7] K. L. Clarkson and K. Varadarajan. Improved Approximation Algorithms for Geometric Set Cover, In Proceedings of *ACM Annual Symposium on Computational Geometry,* 2005.
[8] Q. Cao, T. Yan, J. A. Stankovic and T. F. Abdelzaher. Analysis of Target Detection Performance for Wireless Sensor Networks. In *Proc. of DCOSS,* 2005.
[9] T. Gonzalez. Covering a Set of Points in Multidimensional Space. *Information Processing Letters,* vol. 30, no. 1, 1991.
[10] D. S. Hochbaum and W. Maass. Approximation Schemes for Covering and Packing Problems in Image Processing and VLSI. *Journal of the ACM,* vol. 32, no. 1, 1985.
[11] R. Iyengar, K. Kar and S. Banerjee. Low-coordination Topologies for Redundancy in Sensor Networks. In *Proc. of ACM MobiHoc,* 2005.
[12] R. Kershner. The Number of Circles Covering a Set. *American Journal of Mathematics,* vol. 61, 1939.
[13] S. Kumar, T. H. Lai, and J. Balogh. On k-Coverage in a Mostly Sleeping Sensor Network. In *Proc. of ACM MobiCom,* 2004.
[14] S. Kumar, T. H. Lai, and A. Arora. Barrier Coverage With Wireless Sensors. In *Proc. of ACM MobiCom,* 2005.
[15] J. B. M. Melissen and P. C. Schuur. Improved Coverings of a Square with Six and Eight Equal Circles. *Electronic Journal of Combinatorics,* vol. 3, no. 1, 1996.
[16] S. Megerian, F. Koushanfar, G. Qu, G. Veltri and M. Potkonjak. Exposure in Wireless Sensor Networks: Theory and Practical Solutions. *Wireless Networks,* vol. 8, no. 5, 2002.
[17] K. J. Nurmela and P. R. J. Östergård. Covering a Square with Up to 30 Equal Circles. *Research Report A62,* Laboratory for Theoretical Computer Science, Helsinki University of Technology, 2000.
[18] G. F. Toth. Covering with Fat Convex Discs. *Journal of Discrete and Computational Geometry,* vol. 34, no. 1, 2005.
[19] http://www.xbow.com.
[20] http://www.wolfautomation.com.
[21] http://samraksh.com.
[22] http://zuff.info/RangeFinderCOmp_E.html.
[23] Y. Zhou and K. Charkrabarty. Sensor Deployment and Target Localization Based on Virtual Force. In *Proc. of IEEE INFOCOM,* 2003.
[24] M. Zuniga and B. Krishnamachari. Analyzing the Transitional Region in Low Power Wireless Links. *Technical Report.* University of Southen California, 2004.
[25] J. Zhao and R. Govindan. Understanding Packet Delivery Performance in Dense Wireless Sensor Networks. In *Proc. of ACM SenSys,* 2003.